

SUPPORTING MATERIALS

Kinesin-2 KIF3AC and KIF3AB Can Drive Long Range Transport along Microtubules

Stephanie Guzik-Lendrum^{1,a}, Katherine C. Rank^{2,a}, Brandon M. Bense¹, Keenan C. Taylor²,

Ivan Rayment^{2,*}, and Susan P. Gilbert^{1,*}

¹Department of Biological Sciences and Center for Biotechnology and Interdisciplinary Studies,
Rensselaer Polytechnic Institute, Troy, NY 12180 USA

²Department of Biochemistry, University of Wisconsin, Madison, WI 53706 USA

SUPPORTING MATERIALS

Materials and Methods

2 figures

8 movies

SUPPLEMENTAL MATERIALS AND METHODS

Protein expression and purification

All KIF3 dimers used in this report were expressed in *E. coli* BL21-CodonPlus (DE3)-RIL cells (Stratagene Corporation, La Jolla, CA) with heterodimers resulting from co-transformation of two plasmids and selection on lysogeny broth (LB) plates containing 100 µg/ml ampicillin, 50 µg/ml kanamycin, and 10 µg/ml chloramphenicol. Positive clones were selected and grown in LB medium with antibiotics at 37°C to an A_{600} of ~0.5. Expression was induced by addition of 0.2 mM isopropyl β-D-1-thiogalactopyranoside (IPTG) with shaking at 185 rpm at 16°C for ~15 h. The cells were collected by centrifugation and resuspended followed by gentle stirring at 4°C for 30 min at 1 g cells per 10 ml buffer (10 mM sodium phosphate buffer, pH 7.2, 300 mM NaCl, 2 mM MgCl₂, 0.1 mM EGTA, 10 mM PMSF, 1 mM DTT, 0.2 mM ATP, and 30 mM imidazole plus 0.1 mg/ml lysozyme). Cell lysis was achieved by three replicate cycles of freezing in liquid N₂ and thawing in a 37°C water bath. The lysate was clarified by ultracentrifugation and applied to a HisTrap FF Ni²⁺-NTA column (GE Healthcare, Piscataway, NJ) that was pre-equilibrated with Ni²⁺-NTA binding buffer (20 mM sodium phosphate buffer, pH 7.2, 300 mM NaCl, 2 mM MgCl₂, 0.1 mM EGTA, 1 mM DTT, 0.2 mM ATP, and 30 mM imidazole). The loaded column was washed with binding buffer until baseline absorbance was reached, and protein was eluted with a linear gradient (Ni²⁺-NTA binding buffer: 30 mM imidazole to 300 mM imidazole, pH 7.2). For heterodimeric KIF3 proteins, positive Ni²⁺-NTA fractions were pooled and transferred to a StrepIIactinTM column (StrepTrapII HP, GE Healthcare) pre-equilibrated with StrepII column buffer (20 mM sodium phosphate buffer, pH 7.2, 300 mM NaCl, 2 mM MgCl₂, 0.1 mM EGTA, 1 mM DTT, 0.2 mM ATP). The loaded column was washed with the StrepII column buffer to return the absorbance to baseline, followed by elution (StrepII column buffer plus 2.5 mM desthiobiotin). Following StrepII elution, heterodimeric fractions were examined by SDS-PAGE and only fractions containing a 1:1 ratio of each KIF3 polypeptide were selected, pooled, concentrated, and dialyzed at 4°C overnight in 20 mM HEPES, pH 7.2 with KOH, 0.1 mM EDTA, 5 mM magnesium acetate, 50 mM potassium acetate, 1 mM DTT, 5% sucrose, 100 mM NaCl.

For homodimeric motors, fractions from the HisTrap FF Ni²⁺-NTA column were pooled, concentrated, and further purified by gel filtration on an HPLC gel filtration column (SuperoseTM 10/300, GE Healthcare Life Sciences, Piscataway, NJ) using a Beckman Coulter System Gold HPLC (Fullerton, CA) with elution in 20 mM HEPES, pH 7.2, with KOH, 0.1 mM EDTA, 0.1 mM EGTA, 5 mM magnesium acetate, 50 mM potassium acetate, 1 mM DTT plus 100 mM NaCl. Elution was determined by intrinsic fluorescence detection (Jasco FP-2020, Victoria, British Columbia). All purified proteins were clarified by ultracentrifugation, and the homodimer or heterodimer state was additionally confirmed by analytical gel filtration and SDS-PAGE (Fig. 2). Typical yields for purified motors from bacterial expression were 1.7-3 mg/g *E. coli*. Note that the purification tags were not cleaved for the experiments reported herein.

Steady-state ATPase assays

The steady-state ATPase experiments (Fig. 6) were conducted by measuring the kinetics of the conversion of [α-³²P]ATP to [α-³²P]ADP•P_i as described previously (35, 69). Microtubule-

dependent experiments were performed using 0.1 μM KIF3 active sites, 2 mM MgATP and trace [$\alpha\text{-}^{32}\text{P}$]ATP, plus varying microtubule concentrations that were stabilized with 40 μM paclitaxel in ATPase buffer. Because the KIF3 protein concentration was not 10-fold lower than the $K_{1/2,MT}$, a quadratic function was fit to the data of the observed rates of ATP turnover plotted as a function of microtubule concentration:

$$\text{Rate} = 0.5 * (k_{cat}/E_0) \left[(E_0 + K_{1/2,MT} + MT_0) - \left((E_0 + K_{1/2,MT} + MT_0)^2 - (4E_0MT_0) \right)^{1/2} \right]$$

where Rate (s^{-1}) is expressed as μM ADP \cdot P $_i$ produced per second per ATP binding site, and k_{cat} is the maximum rate constant of steady-state ATP turnover. E_0 represents the ATP binding site concentration (μM), MT_0 is the concentration of tubulin polymer (μM), and $K_{1/2,MT}$ is the MT concentration that provides one-half the maximum rate of steady-state ATP turnover.

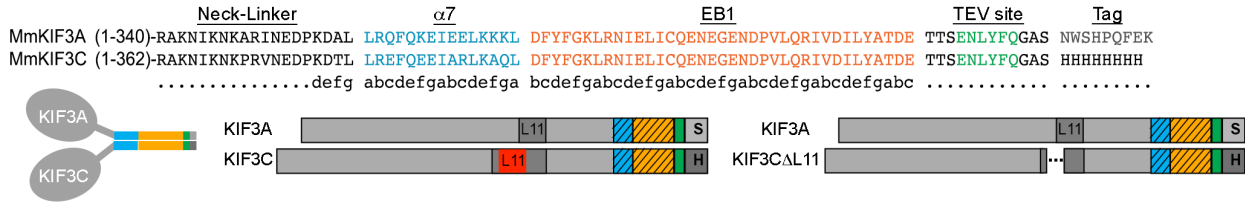
ATP-dependent steady-state experiments were performed using 0.1 μM KIF3 active sites and 20 μM microtubules stabilized by 40 μM paclitaxel in ATPase buffer with varying concentrations of MgATP plus trace [$\alpha\text{-}^{32}\text{P}$]ATP. Observed rates were plotted as a function of increasing MgATP concentration, and the fit of the Michaelis-Menten equation to the data provided the k_{cat} and $K_{M,ATP}$.

For each KIF3 motor, the mean value \pm SEM for the k_{cat} parameter was obtained by compiling data from both the microtubule- and ATP-dependent data sets (N=4-6). The mean value \pm SEM for the $K_{M,ATP}$ parameter was obtained by compiling data from the ATP-dependent data sets (N=2-3), and the mean value \pm SEM for the $K_{1/2,MT}$ parameter was obtained by compiling data from microtubule-dependent data sets (N=2-3).

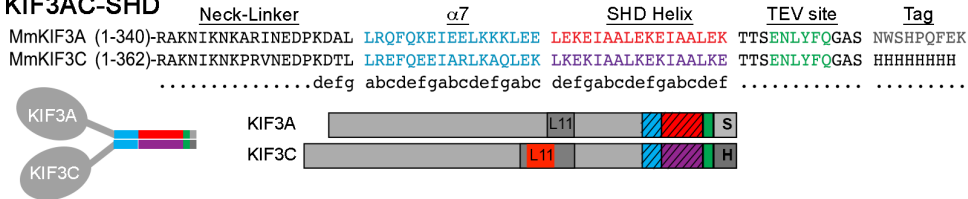
***In vitro* microtubule gliding assays**

Polarity marked rhodamine-labeled microtubules were polymerized as described (70) and stabilized with 20 μM paclitaxel. Microtubule•motor complexes were preformed with 1 mM AMPPNP (final concentration 500 nM tubulin polymer and 2.5 μM kinesin dimer). For microtubule gliding perfusion chambers using acid-washed coverslips were initially coated with 50 mg/ml Penta-His antibody (Qiagen, Valencia, CA) for 10 min followed by a 5 min incubation of blocking buffer (PME80, 1.5 mM magnesium acetate, 0.25 mg/ml casein, 25 mM glucose, 0.2 mg/ml glucose oxidase, 175 $\mu\text{g}/\text{ml}$ catalase, 0.3 mg/ml creatine phosphokinase, 2 mM phosphocreatine, 15 μM paclitaxel, and 1 mM AMPPNP). Microtubule•motor complexes were then introduced into the chamber and were allowed to bind for 5 min. Unbound complexes were then washed out with excess blocking buffer. Surface-bound motors were then activated by introducing activity buffer (blocking buffer supplemented with 1.5 mM MgATP). Microtubule gliding was imaged by TIRF microscopy at 564 nm using 180-ms exposure time and a 20 s interval for 15 min at 25°C. The velocity of gliding microtubules (Fig. 2E) was determined by tracking the leading edge of the moving polarity-marked microtubules (3-7 μm long) using the tracking algorithm on AxioVision 4.8.2 software (Carl Zeiss Microscopy, Inc.). Microtubule gliding velocity data were then compiled, and a Gaussian fit of the histogram determined the mean velocity \pm SEM.

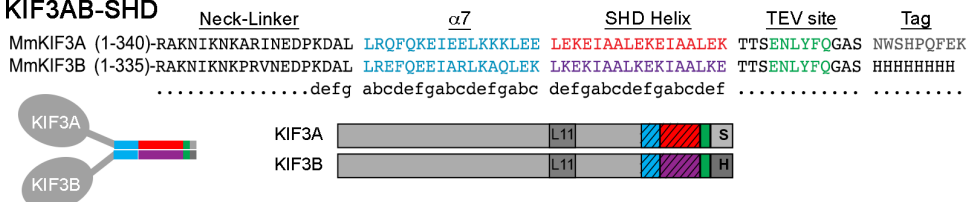
KIF3AC-EB1 and KIF3ACΔL11-EB1



KIF3AC-SHD



KIF3AB-SHD



KIF3AA-EB1



KIF3BB-EB1



KIF3CC-EB1 and KIF3CCΔL11-EB1



Figure S1. Illustration of KIF3 dimeric motors, related to Figures 1 and 2.

All motors expressed in these experiments contain an N-terminal motor and neck linker with the full native sequence of helix $\alpha 7$ fused in-register with either the coiled-coil dimerization domain of EB1 or a synthetic heterodimerization domain sequence (SHD), followed by a TEV protease-cleavage site flanked by linker sequence and C-terminal affinity purification tags (See also Fig. 1). For heterodimeric proteins, two tags were employed that are specific to each motor (S, StrepII tag; H, His₈ tag) to ensure purification of heterodimeric KIF3 motors.

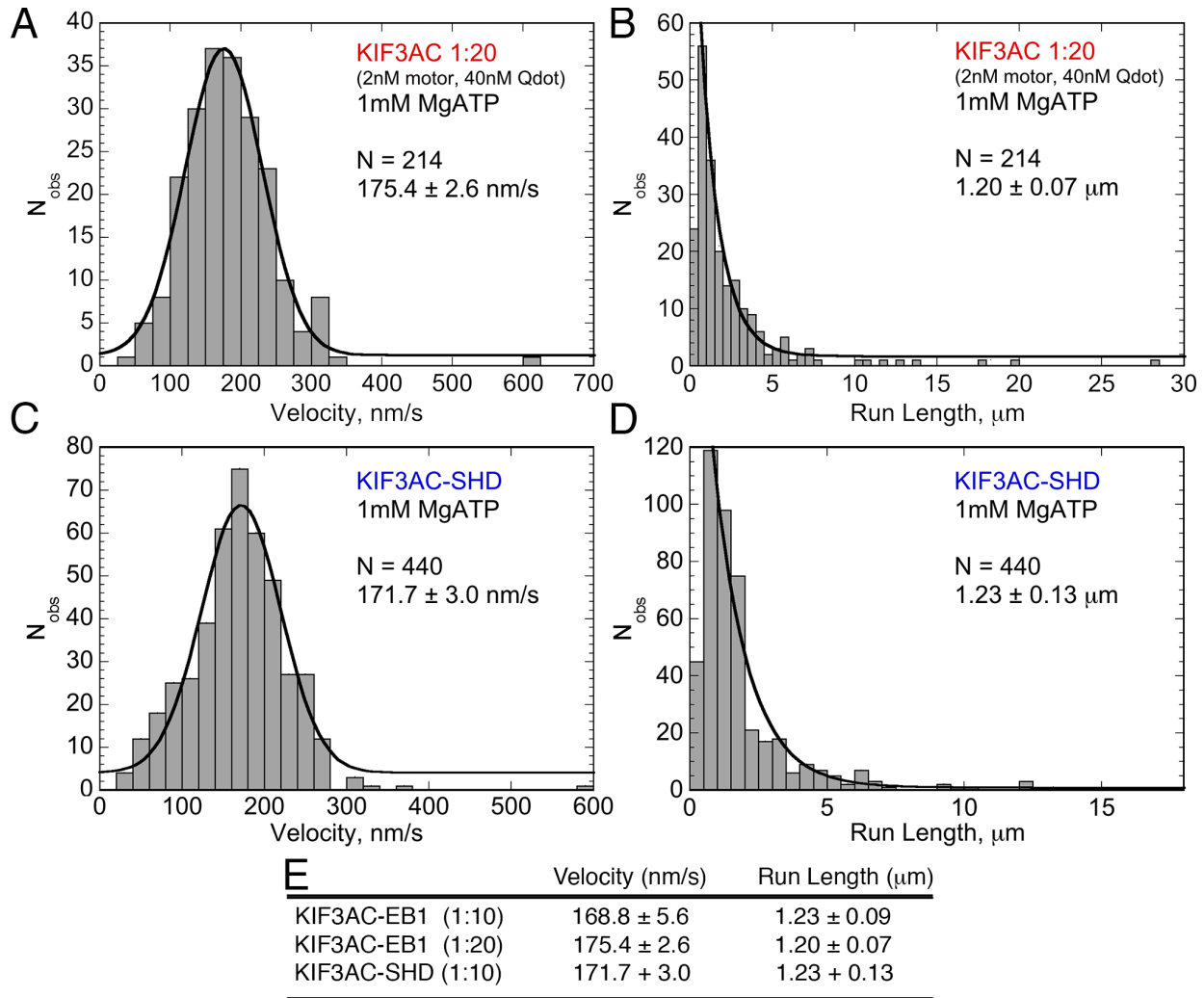
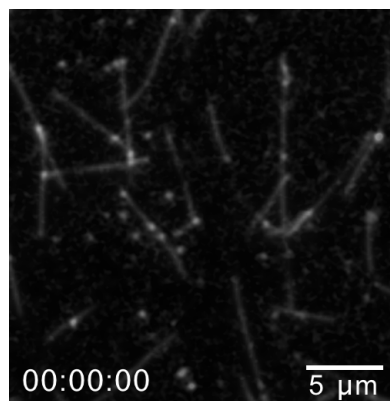


Figure S2. Alternative assays testing the experimental design, related to Figure 3.

(A and B) Histograms of velocity (A) and run length (B) of KIF3AC-EB1 in 1 mM MgATP performed at a 1:20 ratio of KIF3 dimer:Qdot to enhance the probability of examining motors in the single molecule regime. At this ratio, a Poisson distribution would predict 4.8% of Qdots bound by single motors, and 0.1% of Qdots bound by two motors. (C and D) Histograms of velocity (C) and run length (D) of KIF3AC-SHD in 1 mM MgATP performed at the standard 1:10 ratio of dimer:Qdot. (E) Table of compiled data comparing KIF3AC-EB1 (Fig. 3A) to the two alternative assays. Results from Qdot analyses indicate that there is no statistically significant difference between the velocities and run lengths of KIF3AC motors at 1:10 and 1:20 ratios, confirming that the single molecule regime is achieved in the standard 1:10 ratio used herein. Additionally, the use of the coiled-coil dimerization domain of EB1 does not enhance run length of KIF3AC compared to motors dimerized with a synthetic heterodimerization domain motif (SHD).

Movies S1-S8. Videos of representative KIF3 single molecule experiments.

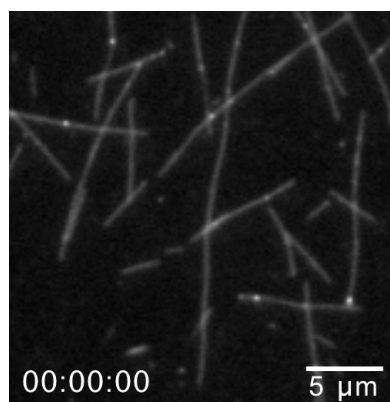
Movie S1: K560



Representative video of kinesin-1 K560 at 1.5 mM MgATP.

Average velocity 305.1 nm/s, mean run length 1.26 μm (See also [Fig. 3C](#)). Video playback speed at 20x real-time.

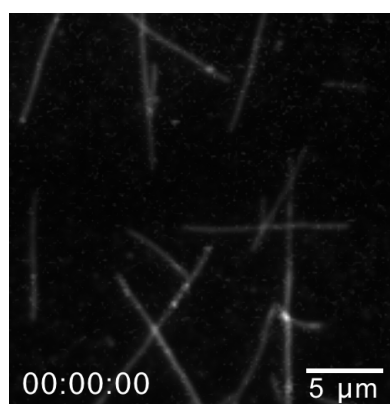
Movie S2: KIF3AC



Representative video of KIF3AC at 1 mM MgATP.

Average velocity 168.8 nm/s, mean run length 1.23 μm (See also [Fig. 3A](#)). Video playback speed at 20x real-time.

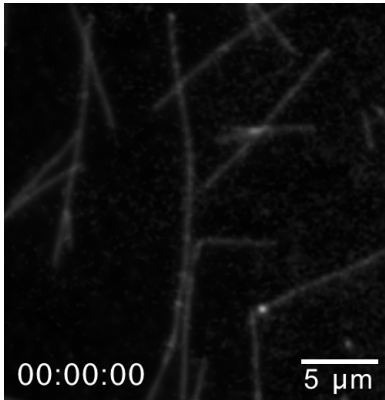
Movie S3: KIF3AB



Representative video of KIF3AB at 1 mM MgATP.

Average velocity 224.5 nm/s, mean run length 1.62 μm (See also [Fig. 3B](#)). Video playback speed at 20x real-time.

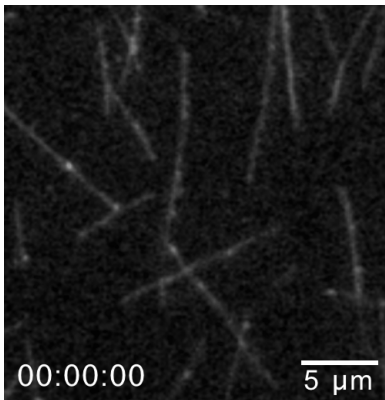
Movie S4: KIF3AC Δ L11



Representative video of KIF3AC Δ L11 at 1 mM MgATP.

Average velocity 171.5 nm/s, mean run length 1.52 μ m (See also [Fig. 4C](#)). Video playback speed at 20x real-time.

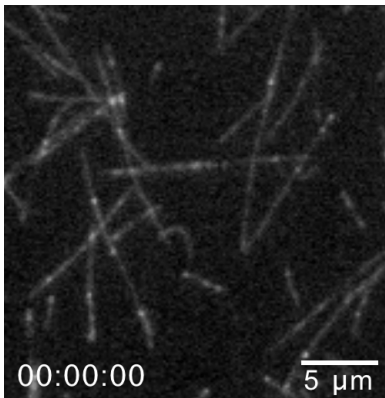
Movie S5: KIF3CC



Representative video of KIF3CC at 1 mM MgATP.

Average velocity of 7.5 nm/s, mean run length 0.57 μ m (See also [Fig. 5A](#)). Timeframe of video is 30 min, with playback speed at 360x real-time.

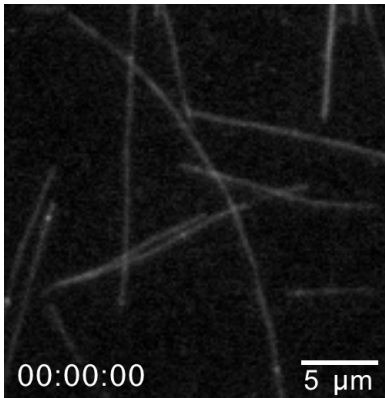
Movie S6: KIF3CC Δ L11



Representative video of engineered homodimeric KIF3CC Δ L11 at 1 mM MgATP.

Average velocity 7.5 nm/s, mean run length 0.75 μ m (See also [Fig. 5B](#)). Timeframe of video is 30 min, with playback speed at 360x real-time.

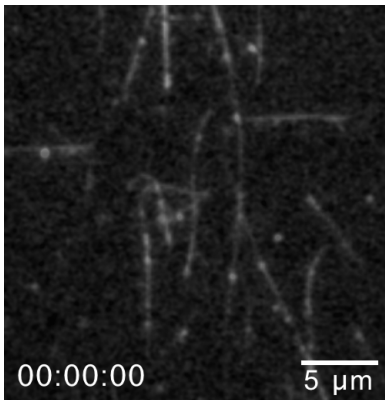
Movie S7: KIF3AA



Representative video of engineered homodimeric KIF3AA at 1 mM MgATP.

Average velocity 239.2 nm/s, mean run length 0.98 μm (See also [Fig. 5C](#)). Video playback speed at 20x real-time.

Movie S8: KIF3BB



Representative video of engineered homodimeric KIF3BB at 1 mM MgATP.

Average velocity 327.6 nm/s, mean run length 1.51 μm (See also [Fig. 5D](#)). Video playback speed at 20x real-time.

SUPPLEMENTAL REFERENCES

69. Gilbert, S. P., and A. T. Mackey. 2000. Kinetics: a tool to study molecular motors. *Methods*. 22:337-354.
70. Sardar, H. S., V. G. Luczak, M. M. Lopez, B. C. Lister, and S. P. Gilbert. 2010. Mitotic kinesin CENP-E promotes microtubule plus-end elongation. *Curr. Biol*. 20:1648-1653.